Step Edge Diffusion and Step Atom Detachment in Surface Evolution: Ion Erosion of Pt(111)

Thomas Michely,[1,*] Matthias Kalff,[2,†] George Comsa,[3] Matthias Strobel,[1,4,‡] and Karl-Heinz Heinig[4]

[1]*I. Physikalisches Institut, RWTH-Aachen, 52056 Aachen, Germany*

[2]*Institut für Grenzflächenforschung und Vakuumphysik, Forschungszentrum Jülich, 52425 Jülich, Germany*

[3]*Institut für Theoretische und Physikalische Chemie, Universität Bonn, 53115 Bonn, Germany*

[4]*Institut für Ionenstrahlphysik und Materialforschung, Forschungszentrum Rossendorf, 01314 Dresden, Germany*

(Received 29 August 2000)

The temperature dependent morphological evolution of Pt(111) under 1 keV Xe^+ normal incidence ion bombardment has been investigated up to 600 monolayers removed. Coarsening of the surface structures during erosion and a qualitative change in roughness evolution between 650 and 700 K are found to be caused by different atomic processes: the former by diffusion of atoms along steps, the latter by the onset of step atom detachment.

DOI: 10.1103/PhysRevLett.86.2589 PACS numbers: 68.35.Bs, 61.80.Jh, 68.35.Fx

Destabilization of an initially smooth surface by homoepitaxial growth or by ion erosion has become a topic of intense experimental and theoretical research (e.g., [1–15]). For low index crystal surfaces and normal particle incidence destabilization results in a morphology of mounds and/or pits. Asymmetries of incorporation into ascending and descending steps for adatoms and vacancies have been identified as key mechanisms of surface destabilization [1,2]. The surface destabilization is frequently [6,7,9], though not always [11], accompanied by coarsening of the surface structure, i.e., an increase in the separation of the characteristic surface features. Phenomenological theory [4,10,15] assumes coarsening to rely on a surface diffusion current $\mathbf{j}_{\mathrm{eq}} \sim \nabla(\nabla^2 h)$ (h is the surface height) driven by curvature dependent differences of the surface chemical potential. Depending on surface crystallography, scaling exponents $1/z$ between $1/4$ and $1/3$ are expected for the coarsening of the characteristic surface length scale λ with removed (or deposited) amount Θ: $\lambda \sim \Theta^{1/z}$ [4,10,15]. For a crystalline surface, diffusion may be due either to detachment of atoms from steps followed by their migration over terraces and subsequent reattachment or to the motion of atoms along step edges. It is *a priori* not clear whether both or only one, and then which one, of these processes may be linked to the above mentioned phenomenological picture. Recent theoretical work stresses the importance of step edge diffusion for coarsening [12–14], while recent experimental work favors step atom detachment [7,9]. In this Letter we report on compelling experimental evidence for the dominance of step edge diffusion for *coarsening* on dense packed crystal surfaces. Step atom detachment is, however, not less important: For the case of ion erosion its onset causes a qualitative change in *roughness* buildup.

The experiments were performed in a variable temperature STM apparatus with a background pressure below 5×10^{-11} mbar. A clean Pt(111) sample with a relative density of step atoms below 1×10^{-3} was prepared prior to each experiment by ion bombardment at 970 K, followed by brief annealing to 1170 K. The differentially pumped ion source supplied a mass selected beam at normal incidence resulting in an erosion rate of 1 monolayer (ML) in 280 s. At the end of bombardment, the sample was cooled to room temperature and imaged by scanning tunneling microscopy (STM). STM images shown here are differentiated images. For large, grey scale topographs the height-height correlation function $G(\mathbf{r}) = \langle h'(\mathbf{x})h'(\mathbf{x} + \mathbf{r})\rangle$ with $h'(\mathbf{x}) = h(\mathbf{x}) - \bar{h}$ was determined, with $h(\mathbf{x})$ the height of the surface at point $\mathbf{x}$ and $\bar{h}$ the mean height. The surface roughness σ is given by $\sigma = \sqrt{G(0)}$. As structure separation we used $\lambda = \frac{1}{2}(\lambda_1 + \lambda_2)$, where λ_1 is the double of the first zero of $G(\mathbf{r})$, i.e., $\lambda_1 = 2|\mathbf{r}_1|$ with $G(\mathbf{r}_1) = 0$, while λ_2 is the quadruple of the full width at half maximum of $G(\mathbf{r})$, i.e., $\lambda_2 = 4|\mathbf{r}_2|$ with $G(\mathbf{r}_2) = \frac{1}{2}G(0)$.

Figures 1a–1d exhibit STM topographs after removal of various amounts at 600 K. The morphology develops from monolayer deep compact vacancy islands to regular hexagonal pits consisting of stacked vacancy islands and remainder pyramids and ridges in between. This evolution is driven by preferential nucleation of new vacancy islands at the bottom of existing ones. Figures 1e–1h exhibit STM topographs (note the different scale) after removal of similar amounts, but at 750 K. In contrast to erosion at 600 K, at 750 K initially vacancy islands coalesce prior to nucleation of new vacancy islands on bottom terraces. Roughness builds up only slowly by remainders of coalesced layers (Figs. 1f and 1g). As steps cannot pass by steps, these remainders pin steps also in subsequently eroded, deeper layers (Fig. 1g) and eventually pits with large flat bottoms result (Fig. 1h). The large difference in roughness evolution at the two temperatures is also apparent in the quantitative data of Fig. 2. At 600 K roughness increases rapidly with Θ and for $\Theta > 10$ ML a scaling exponent $\beta = 0.34 \pm 0.03$ ($\sigma \sim \Theta^{\beta}$) is obtained from linear regression to the data. Although at 750 K and for $\Theta > 10$ ML roughness increases faster than at 600 K (signified by $\beta = 0.57 \pm 0.02$), due to the delay in roughness buildup the absolute values of roughness remain lower. The temperature dependent switch in roughness evolution

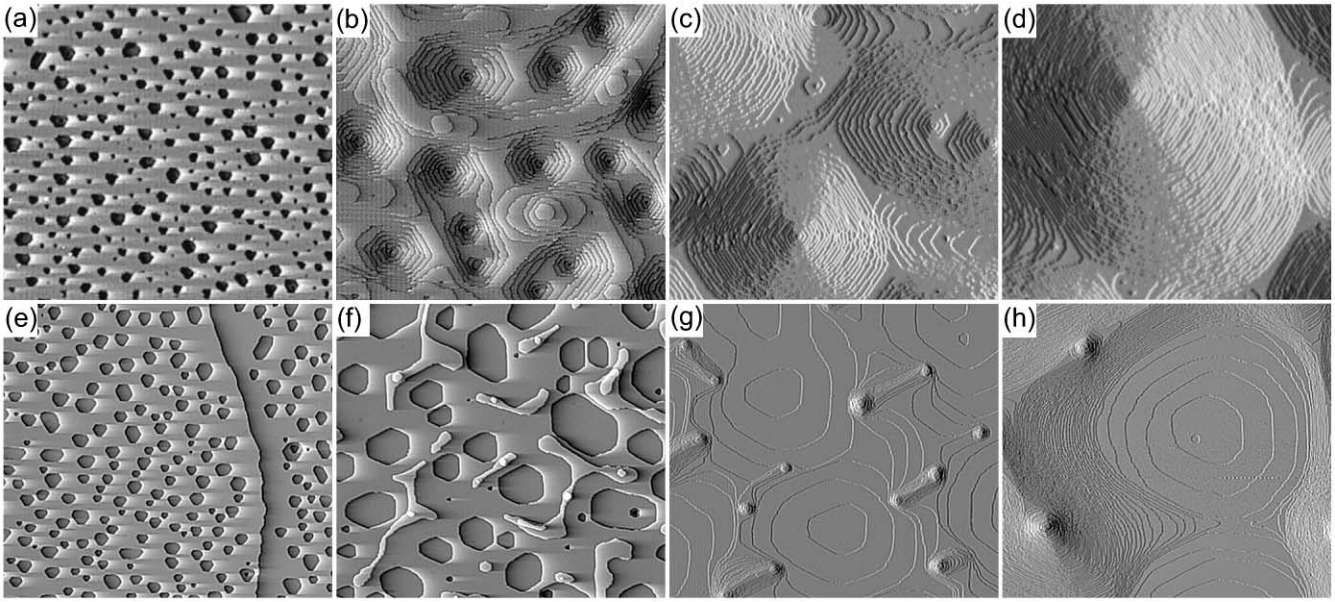

FIG. 1. STM topographs after erosion of (a) 0.26 ML, (b) 6.2 ML, (c) 66 ML, and (d) 333 ML at 600 K and of (e) 0.24 ML, (f) 6.3 ML, (g) 65 ML, and (h) 601 ML at 750 K. Topograph width 810 Å for (a)–(d) and 3460 Å for (e)–(h).

is located between 650 and 700 K, as is indicated by the rise from $\beta = 0.40 \pm 0.03$ at 650 K to $\beta = 0.58 \pm 0.03$ at 700 K. In contrast to roughness evolution, it is seen directly on the topographs of Fig. 1 and from the quantitative data in Fig. 2 that coarsening follows the same rule at 600 and 750 K. In fact, for $\Theta > 10$ ML and the investigated temperatures of 600, 650, 700, and 750 K a common coarsening exponent $1/z = 0.28 \pm 0.02$ is obtained.

Destabilization.—Each 1 keV Xe^+ ion impact sputters away about three atoms and creates eight surface vacancies as well as five adatoms surrounding the vacancies [16]. On a step-free surface annealing of the mobile adatoms with the mobile vacancies leaves only some of the majority point defects (surface vacancies) left, which can nucleate and form vacancy islands as visible in Fig. 1a. It is well known that the incorporation of vacancies into ascending steps is hindered by an effective step edge barrier [1,8,17]. Compared to a step-free terrace, the confinement of the vacancies within vacancy islands therefore increases the nucleation probability and gives rise to pit formation.

Coarsening.—Coarsening of the pits during erosion at 600 K cannot be due to step atom detachment, because step atom detachment becomes relevant on the time scale needed for the removal of one ML only between 650 and 700 K. This can be inferred from Fig. 3. By Pt deposition on Pt(111) at 400 K triangular adatom islands are formed, some of them carrying second layer islands (Fig. 3a). Annealing these islands for 180 s at 630 K leads to hexagonal islands (Fig. 3b). Their number density, the number density of the second layer islands, and the fractional coverage remains constant. Only annealing at 700 K leads to dissociation of nearly all second layer islands (Fig. 3c) [18]. From a quantitative analysis of such annealing experiments an increase in the atom detachment rate by more than 3 orders of magnitude is found between 600 and 750 K, whereas the coarsening behavior in erosion remains unchanged in the same temperature interval. Coarsening of pits and mounds in the present measurements is proposed to be due to efficient step edge diffusion. Rapid step edge

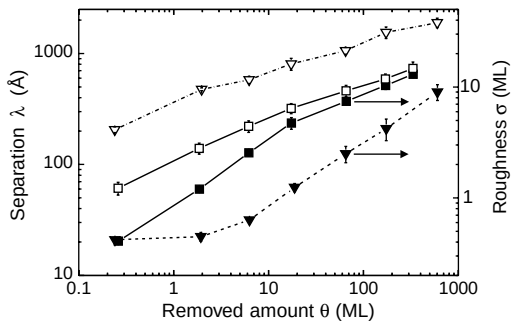

FIG. 2. Feature separation λ (left y-axis) and roughness σ (right y-axis) in dependence of removed amount Θ at 600 K (down triangles and dashed lines) and 750 K (squares and full lines). Full symbols for σ and open symbols for λ. Lines to guide the eye.

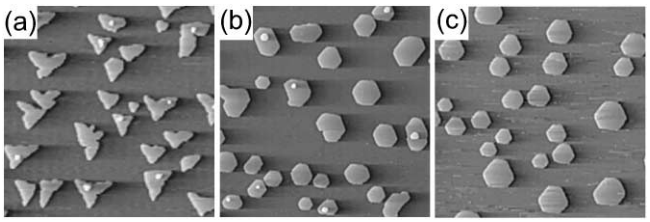

FIG. 3. (a) STM topograph after deposition of 0.2 ML Pt at 400 K. (b) Morphology created as in (a), but after subsequent annealing to 630 K for 180 s. (c) Morphology created as in (a), but after annealing to 700 K for 180 s. Topograph width 2200 Å.

diffusion may be inferred directly from the shape transformation shown in Fig. 3 and the always hexagonal pit shape in Fig. 1. The edge diffusion mechanism for pit coarsening is similar to the one proposed by Tang *et al.* [12] for mound coarsening and is sketched in the cartoons of Fig. 4. After coalescence (Fig. 4a), the line tension of the new common step of the joint island causes the step to approach again a compact shape, enabled by step edge diffusion. Thereby it starts to interact with the two vacancy islands in the bottom terrace, moving them towards their common center of mass (Fig. 4b). The interaction of the steps may be either by material transport between the different layers upon step encounter or by repulsive step-step interactions, which are known to be strong on Pt(111) [19]. Step edge diffusion induced position and shape fluctuations of the bottom layer islands [20] allow them to approach in reaction to the position of the upper layer island. These processes eventually lead to coalescence of the bottom layer vacancy islands prior to nucleation of new islands in both of their bottoms. If after coalescence only one island is left on the bottom terrace, the process is finished: Rapid rearrangement by edge diffusion in all layers will lead to a single pit consisting of stacked hexagonal vacancy islands. Figure 4c shows a typical situation, for which the above described scenario applies.

We performed kinetic 3D lattice Monte Carlo simulations [21] for ion erosion of a fcc(111) surface, including correct numbers for adatoms and vacancies created by single 1 keV Xe^+ impacts and adequate lateral distributions around the impact points. The simulations are performed at 500 K in a linear nearest neighbor model, which reproduces the hierarchy of diffusion processes on Pt(111) adequately. The activation barrier for a process results from the difference in coordination (bond strength 0.25 eV) of initial and final states and an additional fixed kinetic barrier which is 0.6 eV for all processes except adatom diffusion (0.3 eV). The bond strength and kinetic barrier are set to reproduce the annealing experiment of Fig. 3: Within 30 s simulation time a triangular island rearranges into a hexagonal island in the absence of ion bombardment. Step atom detachment is checked to be insignificant during this reshaping. In the accessible range of 6 removed ML the standard simulation mimics adequately the experimental observations with respect to coarsening, roughness evolution, and pit formation. In order to explicitly test for the relevance of step edge diffusion, additional simulations with two different *ad hoc* rules were performed. First, explicit suppression of atom detachment from steps in the simulation does not change coarsening behavior compared to the standard simulation and results in $1/z = 0.22$. Second, kinks were made irreversible traps for atoms. This allows step-adatoms resulting from the bombardment still to migrate along dense packed steps until they are trapped in kink positions, but thermal creation of step-adatoms from kinks is suppressed. This *ad hoc* rule diminished coarsening largely and an exponent of $1/z = 0.09$ resulted. The MC simulation thus indicates as the key process for coarsening the thermal formation of step-adatoms from kinks. In Figs. 4d–4f three snapshots of a typical pit coarsening process are shown. Figure 4d shows two subpits surrounded by three common steps. Periodically the narrow separation between the subpit top layer vacancy islands breaks and the islands rearrange. Immediately before the snapshot of Fig. 4e the last of these breaks took place, finishing pit coalescence. The two coalesced islands are seen in Fig. 4e just in the processes of reshaping. Subsequently all the steps forming the pit approach a more compact, hexagonal shape (Fig. 4f). The animated graphic representation of the full simulation field including several pit coarsening events and all details of the simulation is accessible electronically via Ref. [22].

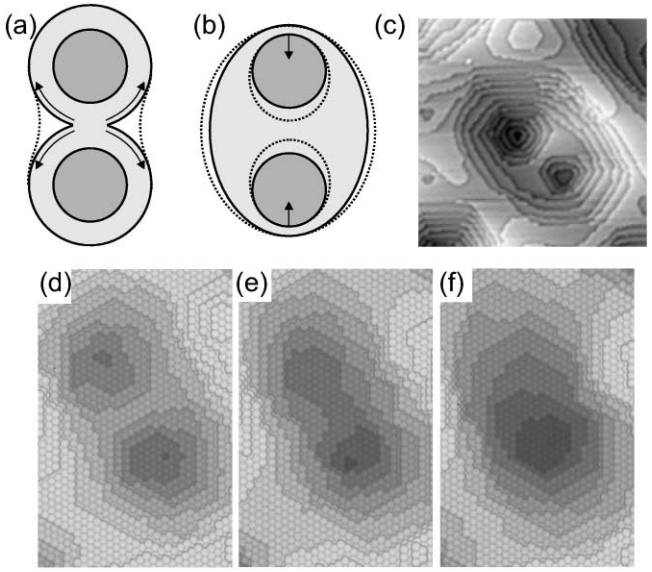

FIG. 4. (a), (b) Schematic sketch for mechanism of coarsening by step edge diffusion (see text). (a) Immediately after coalescence of two vacancy islands a strong edge diffusion current moves material away from the locations of high curvature. (b) During shape rearrangement in response to the step line tension, the coalesced islands approach the two bottom vacancy islands, starting to move them towards their common center of mass. (c) STM topograph of two subpits in the process of coalescence. Topograph width 500 Å, 6.2 ML removed at 600 K. (d)–(f) Snapshots of the MC simulation showing a pit coalescence event. Removed amounts are (d) 3.2 ML, (e) 3.85 ML, and (f) 4.2 ML.

In mound formation during growth of Pt on Pt(111) at 440 K coarsening is largely absent, although the regular mound shapes demonstrate the existence of step edge diffusion. This is straightforward to understand when distinguishing again the different atomic processes involved in step edge diffusion. In fact, at 440 K the morphology freezes entirely in the absence of the deposition flux. Thus thermal formation of step-adatoms from kinks is still absent and accordingly no or only weak coarsening is expected. Nevertheless, adatoms arriving at the step may migrate along steps until they are incorporated at kinks, thus leading to the regular mound shapes (consistent with

the energy barriers derived in [23]). Only at about 500 K step-adatoms are created thermally by emission from kinks [23,24]. These mobile species allow the system to react rapidly to differences in chemical potential along step edges thereby leading to coarsening.

Based on bond counting, for fcc(111) and hcp(0001) surfaces, thermal mobility along step edges, including the formation of step-adatoms and their transport around corners, involves one bond less broken than the thermal formation of adatoms. Therefore one may speculate that the observed coarsening in homoepitaxy on Rh(111) [25] at 725 K and erosion of Au(111) [9] above 295 K is due to step edge diffusion including creation of mobile species rather than step atom detachment. Considering nearest and next nearest neighbor bonding, similar reasoning may be applied to surfaces with square symmetry [e.g., fcc(001)].

Roughness evolution.—The onset of step atom detachment around 700 K, although unimportant for coarsening, is decisive for the roughness evolution. Step atom detachment results in an adatom lattice gas within a vacancy island [17]. The vacancies resulting from ion bombardment are efficiently annealed by this adatom lattice gas (this mechanism mimics a breakdown of the step edge barrier for vacancies). Only when the area of the islands becomes large, the net rate of surface vacancies created exceeds the detachment rate of adatoms from the island step and eventually nucleation takes place. Initially, the lateral length scale does not allow nucleation at the bottom of vacancy islands prior to coalescence. Roughness buildup is therefore delayed (Figs. 1e and 1f). Only the remainders of coalesced layers and the impossibility of steps to pass by these remainders lead gradually to formation of pyramids and ridges, which eventually surround flat areas as seen in Fig. 1h. The delayed initial roughness buildup is a prerequisite to the observed large growth exponents at 700 and 750 K: After the initial delay, for $\Theta > 10$ ML the roughness increases not only by an increase of the separation of the remainder structures while they maintain a fairly constant slope, but also by an increase of the rough area at the expense of the flat area (compare Figs. 1d and 1h). A flat surface may only be maintained forever, if step atom detachment is efficient enough to dissociate remainders of coalesced layers prior to the approach of a new step from a layer below. This condition is much more stringent than the criterion of coalescence prior to nucleation of new bottom islands and has an obvious analog for growth [26].

In conclusion, coarsening of pits in erosion of Pt(111) is due to step edge diffusion including thermal creation of step-adatoms from kink positions. This mechanism is likely to be operative on low index surfaces in erosion as well as growth. Step atom detachment is irrelevant for coarsening, but triggers a transition from pit formation to roughness buildup by remainders of coalesced layers.

We thank Joachim Krug for useful discussions, Michael Hohage for experimental help with Fig. 3, as well as Carsten Busse and Henri Hansen for critically reading the manuscript. One of us (Th. M.) acknowledges support by the Deutsche Forschungsgemeinschaft.

*Corresponding author.
Email address: michely@physik.rwth-aachen.de
†Present address: Continental Teves AG, Guerickestrasse 7, 60488 Frankfurt, Germany.
‡Present address: CNR-INETEM, Stradale Primosole 50, 95121 Catania, Italy.

[1] D. Cherns, Philos. Mag. **36**, 1429 (1977).
[2] J. Villain, J. Phys. I (France) **1**, 19 (1991).
[3] J. Krug, M. Plischke, and M. Siegert, Phys. Rev. Lett. **70**, 3271 (1993).
[4] M. Siegert and M. Plischke, Phys. Rev. Lett. **73**, 1517 (1994).
[5] R. Cuerno and A. L. Barabasi, Phys. Rev. Lett. **74**, 4746 (1995).
[6] J. A. Stroscio *et al.*, Phys. Rev. Lett. **75**, 4246 (1995).
[7] J. K. Zuo and J. F. Wendelken, Phys. Rev. Lett. **78**, 2791 (1997).
[8] B. Poelsema, R. Kunkel, L. K. Verheij, and G. Comsa, Phys. Rev. B **41**, 11 609 (1990); G. Costantini *et al.*, Surf. Sci. **416**, 245 (1998).
[9] M. V. R. Murty *et al.*, Phys. Rev. Lett. **80**, 4713 (1998).
[10] M. Siegert, Phys. Rev. Lett. **81**, 5481 (1998).
[11] M. Kalff, P. Šmilauer, G. Comsa, and Th. Michely, Surf. Sci. Lett. **426**, L447 (1999).
[12] L. H. Tang, P. Šmilauer, and D. D. Vvedensky, Eur. Phys. J. B **2**, 409 (1998).
[13] S. Schinzer, M. Kinne, M. Biehl, and W. Kinzel, Surf. Sci. **439**, 191 (1999).
[14] J. Amar, Phys. Rev. B **60**, R11 317 (1999).
[15] D. Moldovan and L. Golubovic, Phys. Rev. E **61**, 6190 (2000).
[16] Th. Michely and C. Teichert, Phys. Rev. B **50**, 11 156 (1994); M. Morgenstern, Th. Michely, and G. Comsa, Philos. Mag. A **79**, 775 (1999).
[17] Th. Michely, T. Land, U. Littmark, and G. Comsa, Surf. Sci. **272**, 217 (1992).
[18] Note that the step edge barrier for adatoms is negligible for the descent from a hexagonal island: P. J. Feibelman, Phys. Rev. Lett. **81**, 168 (1998).
[19] E. Hahn *et al.*, Phys. Rev. Lett. **72**, 3378 (1994).
[20] G. Rosenfeld, K. Morgenstern, M. Esser, and G. Comsa, Appl. Phys. A **69**, 489 (1999).
[21] M. Strobel, K.-H. Heinig, and Th. Michely, Nucl. Instrum. Methods Phys. Res., Sect. B (to be published).
[22] http://www.fz-rossendorf.de/FWI/FWIT/ion_eros.htm.
[23] P. J. Feibelman, Phys. Rev. B **60**, 4972 (1999).
[24] M. Giesen, G. Schulze Icking-Konert, D. Stapel, and H. Ibach, Surf. Sci. **366**, 229 (1996).
[25] F. Tsui, J. Wellman, C. Uher, and R. Clarke, Phys. Rev. Lett. **76**, 3164 (1996).
[26] More details will be given in M. Kalff, G. Comsa, and Th. Michely (to be published).